The potential of cellular network infrastructures for sudden rainfall monitoring in dry climate regions

N. David[1], P. Alpert[2] and H. Messer[3]

[1] The Department of Geophysical, Atmospheric and Planetary Sciences, Tel-Aviv University, Tel Aviv, Israel.

[2] The Porter School of Environmental Studies and the Department of Geophysical, Atmospheric and Planetary Sciences Tel-Aviv University, Tel Aviv, Israel.

[3] The School of Electrical Engineering, Tel-Aviv University, Tel Aviv, Israel

Corresponding author: Noam David, The Department of Geophysical, Atmospheric and Planetary Sciences, Tel-Aviv University, Ramat Aviv, Tel Aviv, Israel, 69978

Tel: 972-52-8478737

Fax: 972-3-6409282

E-mail: noamda@post.tau.ac.il

Abstract

Monitoring of precipitation and in particular sudden rain, in rural dry climate regions, is a subject of great significance in several weather related processes such as soil erosion, flash flooding, triggering epidemics and more. The rainfall monitoring facilities in these regions and as a result precipitation data are, however, commonly, severely lacking. As was recently shown, cellular networks infrastructures supply high resolution precipitation measurements at ground level while often being situated in dry areas, covering large parts of these climatic zones. The potential found in these systems to provide early monitoring and essential precipitation information, directly from arid regions, based on standard measurements of commercial microwave links, is exemplified here over the Negev desert, South Israel.

We present the results of two different rainfall events occurred in this region. It is shown that the microwave system measured precipitation between at least 50 minutes (in case 1) and at least 1 hour and 40 minutes (in case 2) before each of the sparse rain gauges. During each case, the radar system, located relatively far from the arid sites, provided measurements from heights of at least 1500 m and 2000 m above surface, respectively. A third case study demonstrates the relative advantage of microwave links to measure precipitation intensity in respect to the radar system, over an area of complex topography located in northeastern Israel, relatively far (~150 km) from the radar.

Key words: Microwave links, rainfall, dry climate regions

1. Introduction

Dry climate, which can be further classified into arid and semi arid climate types, cover more than a quarter of the world's land area (Ahrens, 2003; Morin et al., 2009). However, precipitation data from these climatic environments, typified by severe water-scarcity, are severely lacking in comparison to more inhabited regions. Real time rainfall monitoring in such areas is of high importance from several different points of view. Although the total precipitation amounts in dry regions are low, the percentage of intensive rainfall events, generated by severe convection, is major. At the same time, in addition to precipitation, shallow soil with sparse vegetation, a quick decay of the infiltration curve, areas of bare rock, and large inclines of the ravines lead to high levels of peak flow and to the eruption of flash floods (e.g. Cohen et al., 2010, Greenbaum et al., 2006).

Moreover, as a result of the combination of these conditions, the soil erosion due to water is particularly high comparing to other climatic zones. Accelerated erosion by water (and wind) in dry regions is one of the causes of desertification and it exacerbates soil degradation (e.g. Lal, 2001). In addition, especially in warm semi arid and desert fringe regions, precipitation plays a significant role as a factor triggering epidemics (Grover-Kopec et al., 2005). Finally, it has been shown that rainfall patterns have a strong impact on vegetation related processes as well as on the entire (arid and semi arid) ecosystems (e.g. Lazaro et al., 2001; Rietkerk et al., 2002).

_____

Abbreviations: RSL: Received Signal Level, QPE: Quantitative Precipitation Estimates, DSD: Drop Size Distribution, IMS: Israel Meteorological Service, LT: Local Time

On the other hand, desert areas, such as those presented in this research, are particularly problematic for monitoring as the current measuring methods, if existing at all, provide only very limited precipitation data. State of the art rainfall observation systems include surface stations (rain gauges), weather radiosondes and remote sensing systems - radars and satellites. However, these techniques are expensive, not widespread and are often insufficient in their accuracy or in temporal/spatial resolution, especially close to the ground.

Conventional rain gauges, found at surface stations, provide an accurate measurement, but they measure locally, at a single point. In addition, the sparse deployment in dry areas cannot precisely represent precipitation change spatially in stormy rain events (e.g. Michaud and Sorooshian, 1994). Even if the number of gauges in a specific region was much higher, the ability to detect precipitation in a wide area based on this form of measurement would still be small. The probability that a single convective cell will miss the rain gauge entirely is high. Furthermore, even if precipitation were registered in one of the gauges, the likelihood of that particular gauge representing the maximum rainfall in the region is low.

Remote sensing systems provide a large amount of data over large spatial and temporal spans, and have greatly improved the ability to monitor precipitation in these areas. Of these remote sensing systems, the most common for precipitation measurements is the weather radar (Raghavan, 2003). These systems can provide precipitation data every 5 minutes with a spatial resolution of 1 km^2. The range covered by a typical radar system normally stands at around 30,000 km^2 (Morin et al., 2009).

Advanced weather radars can provide a wide range of detailed information about precipitation and the dynamics of rainstorms, from rainfall intensity and wind velocity, to the type and vertical structure of precipitation (Verlinde et al., 2002). Moreover, weather radars have shown to be useful in extending the predictability of flash floods (e.g. Morin et. al, 2009). Despite this, radar data have had limited quantitative use in meteorological applications, because of errors and uncertainty in the surface precipitation estimates derived from it (Harrison et al., 2000). These errors and uncertainties are the outcomes of several factors, such as: calibration issues, the spatial expansion effect of the radar beam and problems with partial beam filling, problems with beam overshooting (Durden et al., 1998; Gabella et al., 2011) and high sensitivity of the rain rate-reflectivity relation to Drop Size Distribution (DSD) variations (Jameson, 1991). In addition, dry desert areas are quite often not covered by radars.

It is obvious then, that the ideal measurement method would provide data from a wide spatial range, as the radar does, with close proximity to the ground, as is the case with rain gauges, directly from the areas of interest, at low costs. The advantage of the precipitation measurement method using existing microwave networks is that it combines these exact characteristics. Cellular network infrastructure already covers large land areas all over the world, including regions that are difficult to access, such as complex topography, and particularly arid and semi arid zones.

Weather conditions and rainfall in particular affect the electromagnetic radiation, causing attenuation of radio signals. Thus, microwave communication networks are in effect built in monitoring sensors of the environment (Messer et al., 2006). The skill of the method to

measure precipitation (correlation with rain gauges), was found to be higher in respect to that of the radar system.

Microwave links are typically installed at elevations of only a few tens of meters above ground level and as a result their measurements reflect the events close to the surface. In addition, many of these systems provide measurements at high spatial and temporal resolutions. Finally, since the data required by the method are only standard network data, the costs are minimal.

Rainfall monitoring, using microwave links, has been extensively studied over the past few years. These links have been shown to be useful for identifying dry and rainy periods (Chwala et al., 2012, Wang et al., 2012, Rayitsfeld et al., 2012) and for estimating path averaged rain rates (e.g. Leijnse et al., 2007a, 2008; Messer et al., 2006; Messer, 2007; Upton et al., 2005). Reconstruction of rainfall intensity distribution using commercial microwave networks has also been presented (Goldshtein et al., 2009; Zinevich et al., 2008, 2009). Other applications which were demonstrated include: areal evaporation measurements (Leijnse et al., 2007b), humidity monitoring (David et al., 2009, 2011), identification of melting snow (Upton et al., 2007), calibration and correction of radar systems (Krämer et al., 2005; Rahimi et al., 2006) and even monitoring of vegetation characteristics (Hunt et al., 2011). Here we demonstrate the ability to produce Quantitative Precipitation Estimates (QPE) based on standard microwave networks measurements taken directly from arid, rural regions and areas of complex terrain where radar and rain gauge techniques are often insufficient.

2. Method

The interpretation and modeling of atmosphere-induced impairments on radio links have been researched by telecommunication specialists for years. Several models, relating the attenuation rate A (given in dB/km) with the rain intensity R (mm/hr), exist. One accepted approach is the power law model for the attenuation described as (Olsen et al. 1978):

$$A = aR^b$$

Where the constants a and b are functions of frequency, polarization and DSD (Jameson, 1991). Given measurements of the Received Signal Level (RSL), and transmission levels, parameters which are routinely collected by many cellular providers, the rainfall induced attenuation A can be derived and hence the requested rain rate R (Messer et al., 2006). In order to determine the base line level of the microwave measurements the median no-rainfall RSL measurements were chosen separately for each link over a no rain period (of at least two hours) prior to the onset of the event. Then, these measurements were subtracted from those acquired during the rainfall event itself. Finally, wet antenna attenuation correction was applied (Zinevich et al, 2009).

3. Sources of error

Both environmental and instrumental effects are sources of error in estimating path-averaged rainfall for a link. A major source is the baseline uncertainty. Fluctuations of atmospheric humidity are a primary cause of baseline level variations over time, as well as ducting and scintillation effects. Temperature variations affect the analog circuitry of the

transmit and receive units may lead to additional signal variations. In addition, mechanical oscillations, such as those caused by winds moving the microwave antennas or alternately scatterers found close to the propagation path (e.g. moving tree leaves) may also cause variations in the baseline signal (Leijnse et al., 2007b). Baseline uncertainty dominates system quantization error uncertainties, as well as errors resulting from DSD variability along the link. Additional sources include wet antenna effects and spatial variability of rainfall in the vicinity of the link, which affects the accuracy of QPE out of the link path. Extensive research analyzing and quantifying the various sources of perturbations has recently been conducted (Zinevich et al., 2010).

4. The Dead Sea and north Negev regions

The Negev desert, constitutes the southern half of Israel, is an arid climate region extending between the latitudes of 29° North and 31°20 North (Kidron, 2000; Jacobs et al., 2002; Kahana et al., 2002) . The climate found in the area of the Dead sea (which borders with the northeast part of the Negev) spans from arid, in the south part and near its shores, to Mediterranean, semi arid climate, in the north (Cohen and Laronne, 2005; Dayan and Morin, 2006).

Severe convection generates heavy precipitation in these regions while two dominant synoptic systems account for most of the major rainfall events (Dayan and Morin, 2006; Kahana et al., 2002; Krichak et al., 2000). One of these is the Red Sea trough- a tropical synoptic scale system. This barometric trough is accompanied by an upper-level trough which develops over Egypt, providing favorable conditions for the development of severe

convective storms. Alpert et al. (2004) have shown that the frequency of Red Sea troughs was doubled over the last 5 decades. The second synoptic system contributing to rainfall in the area is a Syrian Low - an intense Mediterranean cyclone which is centered over Syria.

In the cases demonstrated below it is shown that the radar system covers the middle of the country, while the arid climate study areas, are in the south. As a result, due to the curvature of the Earth and the radar beam transmission angle, the radar precipitation measurements over these areas are distant from the surface at an elevation of about 2000 m above ground level in the case of the north Negev region. In the southern Dead Sea area, in addition to the aforementioned problem, the radar beam, and particularly the one that is transmitted at the lowest elevation angle (which is targeted at providing precipitation measurements from elevations closer to the ground) is disrupted by the regional topography. The data, from the minimal elevation, acquired in this case, are actually measured at an altitude of about 1500 meters above ground. Therefore, precision of these QPE is doubtful.

5. Results

Three case-studies are presented. Two rainfall events that occurred in the arid region of the southern Judean desert and in the northern part of the Negev. The 3rd case-study is based on a rainfall event occurred in northern Israel over an area of complex topography. The microwave system, spread across the tested regions, provides minimal and maximal measurements per 15 minute intervals for each link. Accordingly, the maximal and

minimal rainfall intensities were derived based on these measurements (Messer et al., 2006). The microwave link values represent the average measurement of several links that are routed over the same physical path. The attenuation measurements of the links were related to rainfall only when attenuation was simultaneously recorded on several links over the same propagation path. Three radar images are presented (Fig.1.A, Fig. 2, Fig. 5.A) while the convective cells in each image are overlaid on a physical map of the region. The color of each cell indicates the QPE according to the scale found to the right of each image.

5.1 Case 1: 24-25 October 2008

There are 32 relatively long microwave links deployed in the first examined region of the southern Judean desert (Fig. 1.A). The system's frequency range is 17-19 GHz with a quantization error of 0.1dB. These links span 6 to 26 kms in length, across an area of approximately 60x30 km^2. All links are installed between 10 and 50 meters above ground level and are spread across seven different physical paths (transmitting more than one link over the same physical path is possible by varying link frequency and polarization). The results presented for this case study are derived from 29 of the 32 microwave links found in the region (In some cases, some links were not employed due to a technical malfunction or lack of data for the particular link). Also presented are measurements from 6 Israel Meteorological Service (IMS) rain gauges located at the examined area. On the night between 24 and 25 October 2008, heavy precipitation fell in the Judean desert and the Negev over short periods of time. Cold air at high altitude and the entrance of humidity from Jordan in the east, created a well developed convective cloud, covering the northeastern Negev, and southern Judean desert (Fig. 1.A).

The IMS rain gauges which are deployed in the area, as well as the network of microwave links are depicted in Fig. 1.A. A convective cell (green) can be seen in the Tamar Fort region. The rainfall in this area was detected by the microwave links in the vicinity long (at least 50 minutes) before the rain gauges in the area as can be seen in Fig. 1 (B-E). The cell did not pass over all the specific point-locations of the rain gauges in the region.

Among the rain gauges: the Sdom gauge was the first to measure precipitation only at 21:50 Local Time (LT). The Rotem plain rain gauge – did not indicate precipitation at all while many of the microwave links located at the area indicated precipitation.

As can be seen from the microwave link measurements (Fig. 1.B-C) the cloud movement, in this case, was from south to north. As a result the relatively southern links were the first to measure precipitation as early as 21:00 LT. Finally, the northernmost links, of Beit Yatir- Shima and Beit Yatir-Arad physical paths, detected precipitation.

A simulation was carried out in order to evaluate the effectiveness of the microwave links in capturing the precipitation in comparison to the rain gauges across the study region.

The locations of the precipitation stations and microwave links in the area were mapped. Random circles of a 5 km radius were inserted into the simulation area to represent the convective cells in the region. In the simulation the cases where the location of a convective cell corresponded with a microwave link below it, were counted. Where several links corresponded with a single convective cell – the occurrence was counted only once.

Similarly, all cases where a convective cell was located above the rain gauges, were enumerated. The simulation was run for 10,000 cases in which 10,000 convective cells

were randomly positioned above the simulation area. The results showed that the probability of detecting a convective cell with the microwave links located in this region was 3.6 times greater than the probability of detecting one using a rain gauge (26.6% against 7.3%, respectively).

5.2 Case 2: 17-18 January 2010

On January 17-18, 2010, the Negev, Arava (and Sinai) regions experienced relatively high levels of precipitation. Several IMS rain gauges deployed in the region measured rainfall levels of 30- 80 mm that, in some cases, equaled the entire yearly average for the region. This event was generated due to a cold air surge in the middle atmospheric layer in conjunction with an equatorial moisture layer below which was advected to the region from central Africa by the sub- tropic jet stream (Ziv, 2001).

Figure 2 presents the radar image acquired at 19:00 LT during January 17.

Figure 3 details the study area including the locations of the microwave links deployed in the site along with two online Meteorological Service rain gauges at this location. In this case, we used the measurements of 4 microwave links located over 2 different physical paths. The lengths of the links ranges between 9.5 and 13.2 kms, and they operate in the 18-23 GHz frequency range with a quantization error of 0.1dB. Links are installed between 27 and 70 meters above ground level.

Figure 4, shows the rain rates as deduced from the microwave links (maximum and minimum) along with the rain gauges measurements.

As early as 16:30 LT, the two links located between Nafha and Mitzpe Ramon (Fig. 3) already started indicating rainfall (of low intensity though). Larger amounts of precipitation can be seen from 18:15, further increasing at 18:15- 18:30. Beginning at

18:30, rain is also measured simultaneously on the Nafha – Lavan mountain links, indicating that, during this time slot, rainfall fell over the specific area of the farm located by the links' intersection point. On the other hand, the Mitzpe Ramon rain gauge started measuring precipitation at 18:10 till 18:30 and again at later times while the Ovda gauge started measuring only at 18:40. Other rain gauges, installed at more remote locations (at distances of about 25 to 50 km) from the test site, have started measuring rainfall also only from 18:40 LT or at later times.

5.3 Case 3: Microwave links vs. radar measurements from a relatively remote area of complex terrain

An advantage of the microwave links over the radar system is demonstrated, based on measurements taken during a rainfall event which took place on 11 December 2010 at the Golan Heights, a volcanic plateau spread over an area of 1040 km^2 (Yom Tov et al., 1995) located on the eastern side of the north Jordan valley (northeastern Israel, as seen in Fig. 5.A), about 150 km away from the radar's location in central Israel. The topographic heights, in this region, range from ~ 2,200 m in the north to below sea level in the south. In this case, the radar beam that is transmitted at the lowest angle reaches an elevation of about 2000 m above sea level at this location. In addition, during this event, the radar rays were propagating through many Cumulonimbus clouds which were found along the propagation path, across a distance of a few tens of km (Fig. 5.A). As a result of these conditions, the radar system underestimated the actual rain rate over the region. Two microwave links transmitting on the same physical path are located in the area. A rain gauge is located 6.5 km from the northern end of the links (Fig. 5.B). We compared the rain rate measurements from the microwave system to the radar measurements under the

13

assumption that the rain gauge describes the ground truth. Each of these methods provides measurements in different ways: The microwave links provide maximum and minimum rain rate measurements every quarter hour. Radar provides measurements of rain rate every five minutes, and the rain gauge measures the amount of rain accumulated in every 10 minute period. Therefore, to allow for a comparison to be made, we chose a common base for the three tools as far as measured time interval, as well as the measured quantity (rain rate). Since the links provide a maximum and minimum measurement every 15 minutes, one can deduce that precipitation was continuous in intervals where the minimum and maximum measurements are both greater than zero. During intervals where only a maximum value was observed – one can deduce that the precipitation occurred for a period of less than 15 minutes. To correlate the rain gauge and microwave measurements, we used the maximum measurements of the links that include measurements of precipitation intervals shorter than 15 minutes. We correlated the measurements over a half hour interval, from which the maximum rain gauge and link measurements, respectively, were chosen. The correlation coefficient derived from a Pearson correlation test (Neter et al., 1996), was 0.85 (based on measurements taken between 04:30 and 18:30 LT). We correlated the radar QPE from the area to the rain gauge measurements, using the same time interval (half hour) and for the same time period (04:30 to 18:30 LT). The maximum reading from the rain gauge every half hour was compared to the maximum radar measurement during that same half hour. The correlation coefficient was 0.2. We then compared the intensity measurements. Figure 5.A shows a radar image taken during the storm event at 13:00 LT. Figure 6 presents the rain rate measured during the entire event, by each of the methods, in the observed area. The

rain gauge measurements can be seen to fall between the minimum and maximum QPE of the links. On the other hand, the radar measurements underestimated the intensity compared to the rain gauge and observed precipitation rates of ~1 mm/hr during the whole storm event.

These results show the great potential of microwave systems to provide reliable rain rate measurements with high resolution from areas where, at times, the radar system does not provide sufficient response.

The disparities between the links measurements to those of the rain gauge are expected, primary due to spatial variability of the rainfall (Zinevich et al., 2010). Additionally, the links provided measurements of the minimal and maximal intensities which were taken instantly while the gauge's intensity rates were derived based on the amount of liquid water that has accumulated inside the instrument during a 10 minute time interval.

6. Summary

Very little work has been carried out regarding precipitation measurements in dry climate regions. Here we have demonstrated that already-existing microwave networks deployed in such areas are able to provide vital, high resolution (spatial and temporal) information. A key challenge in measuring precipitation using varied sources (e.g. rain gauge, radar, microwave links) is the ability to integrate the information received from the different tools in a way that recreates the precipitation field most precisely. Particularly, when each measuring instrument has different sampling and resolution characteristics. Goldshtein et al. (2009), for instance, presented a method to reconstruct rainfall intensity distribution

using commercial microwave links. One of the advantages of the technique they describe is the possibility to easily integrate link measurements with rain gauge data and other sources allowing for improvement of estimation accuracy. An additional example of a method that would allow integration while providing the required synergy is use of Copula models (e.g. Vogl et al., 2012).

The results above suggests that the method described here increases the probability of an early detection of single convective cells typical for these areas, and their associated precipitation, as compared to existing rain gauges. The results of the simulation that was carried out also support this conclusion. Specifically, in the rainfall event on 24 October 2008 (case 1), the microwave links (located between Tzafit to Mirvatz Mountain) detected precipitation 50 minutes prior to the first rain gauge indicating rainfall. In this case, the rain gauge found at Rotem plain area, entirely missed the precipitation. The second case-study, demonstrates the ability to provide precipitation data from a remote region where almost no other monitoring facilities exist, and again, at an earlier time with respect to the only two rain gauges; here, the links detected precipitation at about 1 hour and 40 minutes before the Mitzpe Ramon rain gauge and more than 2 hours before the one located in Ovda. The advantage of using the microwave system comparing to the radar may be considerable, when the radar rays are interrupted along the propagation path or when the convective cells are located too low in the troposphere, to be detected properly by the radar, as demonstrated in the 3rd case. This situation often occurs in dry climate areas which are located relatively far from the radar.

These results highlight the potential of commercial microwave links, particularly in connection to early detection and monitoring of damaging amounts of rainfall. Due to

their climatic and hydrological conditions, dry environments are particularly prone to this dangerous phenomenon and from relatively small convective cells. The Judean and the Negev desert regions, which were dealt with here, are examples of such areas (see, e.g. Cohen and Laronne, 2005; Cohen et al., 2010; Dayan and Morin, 2006; Kahana et al., 2002; Shentsis et al., 2012). Intense rainfall is the main flash floods generating factor and hence the ability to predict this phenomenon highly depends on the availability of QPE taken directly from the flood area.   With their combination of destructive power, incredible speed, and unpredictability, flash floods allow only few opportunities to provide timely warning. Thus, they rank among the most devastating weather related natural disasters. Rain gauge networks in these environments are sparse while radar observations are often insufficient. In other cases, there may be no precipitation measurement equipment at all in these arid/semi-arid regions.   Consequently, QPE information derived from existing microwave networks can provide the complimentary useful input required to successfully cope with this potentially hazardous phenomenon.

References

Ahrens, C.D., 2003. Meteorology today: an introduction to weather, climate, and the environment, seventh ed. Brooks/Cole-Thomson Learning, Pacific Grove, CA.

Alpert, P., Osetinsky, I., Ziv, B., Shafir, H., 2004. Semi-objective classification for daily synoptic systems: Application to the Eastern Mediterranean climate change. Int. J. Climatol. 24, 1001-1011.

Cohen, H., Laronne, J. B., 2005. High rates of sediment transport by flashfloods in the southern Judean Desert, Israel. Hydrol. Process. 19, 1687-1702.

Cohen, H., Laronne, J. B., Reid, I., 2010. Simplicity and complexity of bed load response during flash floods in a gravel bed ephemeral river: A 10 year field study. Water Resour. Res., 46. W11542. Doi:10.1029/2010WR009160.

Chwala, C., Gmeiner, A., Qiu, W., Hipp, S., Nienaber, D., Siart, U., Eibert, T., Pohl, M., Seltmann, J., Fritz, J., and Kunstmann, H., 2012. Precipitation observation using microwave backhaul links in the alpine and pre-alpine region of Southern Germany, Hydrol. Earth Syst. Sci. 16, 2647-2661. Doi: 10.5194/hess-16-2647-2012.

David, N., Alpert, P., Messer, H., 2009. Technical Note: Novel method for water vapour monitoring using wireless communication networks measurements. Atmos. Chem. Phys., 9, 2413-2418. Doi: 10.5194/acp-9-2413-2009.

David, N., Alpert, P., Messer, H., 2011. Humidity measurements using commercial microwave links, in: Khatib, M. (Ed.), Advanced Trends in Wireless Communications. InTech, Croatia, pp. 65-78.

Dayan, U., Morin, E., 2006. Flash flood–producing rainstorms over the Dead Sea: A review. Geol. S. Am. S. 401, 53-62. Doi:10.1130/2006.2401(04).

Durden, S., Haddad, Z., Kitiyakara, A., Li, F., 1998. Effects of non-uniform beam filling on rainfall retrieval for the TRMM precipitation radar. J. Atmos. Ocean. Tech. 15, 635-646.

Gabella, M., Morin, E., Notarpietro, R., Michaelides, S., 2011. Winter precipitation fields in the southeastern Mediterranean area as seen by the Ku- band spaceborne weather radar and two C-band ground based radars. Atmos. Res. 119, 120-130. Doi: 10.1016/j.atmosres.2011.06.001.

Greenbaum, N., Ben-Zvi, A., Haviv, I., Enzel, Y., 2006. The hydrology and paleohydrology of the Dead Sea tributaries. Geol. S. Am. S. 401, 63– 93. Doi: 10.1130/2006.2401(05).

Grover- Kopec, E., Kawano, M., Klaver, R.W., Blumenthal1, B., Ceccato1, P., Connor, S. J., 2005. An online operational rainfall-monitoring resource for epidemic malaria early warning systems in Africa, Malaria J. 4, 6. Doi: 10.1186/1475-2875-4-6

Goldshtein, O., Messer, H., Zinevich, A., 2009. Rain Rate Estimation Using Measurements from Commercial Telecommunications Links. IEEE T. Signal Proces. 57(4), 1616-1625. Doi: 10.1109/TSP.2009.2012554.

Harrison, D., Driscoll, S., Kitchen, M., 2000. Improving precipitation estimates from weather radar using quality control and correction techniques. Meteorol. Appl. 6, 135-144.

Hunt, K. P., Niemeier, J. J., da Cunha, L., K., Kruger, A., 2011. Using cellular network signal strength to monitor vegetation characteristics. IEEE Geosci. Remote. S. 8, 346-349.

Jacobs, A.F.G., Heusinkveld, B.G., Berkowicz, S.M., 2002. A simple model for potential dewfall in an arid region. Atmos. Res. 64, 285- 295.

Jameson, A., 1991. A comparison of microwave techniques for measuring rainfall, J. Appl. Meteorol. 30(1), 32–54.

Kahana, R., Ziv, B., Enzel, Y., Dayan, U., 2002. Synoptic climatology of major floods in the Negev Desert, Israel. Int. J. Climatol. 22, 867-882. Doi:10.1002/joc.766.

Kidron, J.G., 2000. Analysis of dew precipitation in three habitants within a small arid drainage basin, Negev Highlands, Israel. Atmos. Res. 55, 257-270.

Krämer, S., Verworn, H. R., Redder, A., 2005. Improvement of X-band radar rainfall estimates using a microwave link. Atmos. Res. 77(1-4), 278-299.

Krichak, S., Tsidulko, M., Alpert, P., 2000. November 2, 1994, severe storms in the southeastern Mediterranean. Atmos. Res. 53, 45-62.

Lal, R., 2001. Soil degradation by erosion. Land Degrad. Develop.12, 519- 539.

Shentsis. I., Laronne. J., Alpert, P., 2012. Red Sea Trough floods in the Negev, Israel (1964-2007). Hyd. Sci. J. 57 (1), 42-51.

Lazaro, R. Rodrigo, F. S., Gutierrez, L., Domingo, F., Puigdefabregas, J., 2001. Analysis of a 30-year rainfall record (1967- 1997) in semi arid SE Spain for implications on vegetation. J. Arid Environ. 48, 373-395.

Leijnse, H., Uijlenhoet, R. and Stricker, J., 2007a. Rainfall measurement using radio links from cellular communication networks. Water Resour. Res. 43, W03201. Doi: 10.1029/2006WR005631.

Leijnse, H., Uijlenhoet, R. and Stricker, J., 2007b. Hydrometeorological application of a microwave link: 1. Evaporation. Water Resour. Res. 43, W04416. Doi: 10.1029/2006WR004988.

Leijnse, H., Uijlenhoet, R. and Stricker, J., 2008. Microwave link rainfall estimation: Effects of link length and frequency, temporal sampling, power resolution, and wet antenna attenuation. Adv. Water Resour. 31, 1481-1493. doi:10.1016/j.advwatres.2008.03.004

Messer, H., Zinevich, A., Alpert, P., 2006. Environmental monitoring by wireless communication networks. Science. 312, 713. Doi:10.1126/science.1120034.

Messer, H., 2007. Rainfall monitoring using cellular networks. IEEE Signal Proc. Mag. 24, 144.

Michaud, J. D., Sorooshian, S., 1994. Effect of rainfall-sampling errors on simulations of desert flash floods. Water Resour. Res. 30(10), 2765-75. Doi:10.1029/94WR01273.

Morin, E., Jacoby, Y., Navon, S., Bet-Halachmi, E., 2009. Towards flash flood prediction in the dry Dead Sea region utilizing radar rainfall information. Adva. Water Resour. 32, 1066–1076. Doi:10.1016/ j.advwatres.2008.11.011.

Neter, J., Kutner, M. H., Nachtsheim, C., Wasserman, W., 1996. Applied Linear Statistical Models, fourth ed. McGraw Hill, New York.

Olsen, R. L., Rogers, D. V., Hodge, D. B., 1978. The aR^b relation in the calculation of rain attenuation. IEEE T. Antenn. Propag. 26(2), 318–29. Doi:10.1109/TAP.1978.1141845

Raghavan, S., 2003. Radar Meteorology. Kluwer Academic Publishers, Netherlands.

Rahimi, A.R., Holt, A.R., Upton, G.J.G., 2006. Attenuation calibration of an X-band weather radar using a microwave link. J. Atmos. Ocean. Technol. 23(3), 295-405.

Rayitsfeld, A., Samuels, R., Zinevich, A., Hadar, U., Alpert, P., 2012. Comparison of two methodologies for long term rainfall monitoring using a commercial microwave communication system. Atmos. Res. 104-105, 119-129.

Rietkerk, M., Boerlijst, M., van Langevelde, F., HilleRisLambers, R., van de Koppel, J., Kumar, L., Prins, H.H.T., de Roos, A., 2002. Self- organization of vegetation in arid ecosystems. The Americain Naturalist. 160 (4), 524- 530.

Upton, G.J.G., Holt, A.R, Cummings, R.J., Rahimi, A.R., Goddard, J.W.F., 2005. Microwave Links: The future of urban rainfall measurement ?. Atmos. Res. 77 (1- 4), 300-312.

Upton, G.J.G, Cummings, R.J., Holt, A.R., 2007. Identification of melting snow using data from dual-frequency microwave links. IET Microw. Antenna P. 1, 282-288.

Verlinde, J., Moiseev, D., Skaropoulos, N., Heijnen, S., Zwan, F., Russchenberg, H., 2002. Spectral polarimetric measurements in the radar bright band. Proceedings of URSI-

F Open Symposium on Propagation and Remote Sensing, Garmisch-Partenkirchen, Germany, February 2002.

Vogl, S., Laux, P., Qiu, W., Mao, G., Kunstmann, H. 2012. Copula-based assimilation of radar and gauge information to derive bias-corrected precipitation fields. Hydrol. Earth Syst. Sci. 16, 2311-2328. Doi: 10.5194/hess-16-2311-2012

Wang, Z., Schleiss, M., Jaffrain, J., Berne, A., Rieckermann, J., 2012. Using Markov switching models to infer dry and rainy periods from telecommunication microwave link signals. Atmos. Meas. Tech. 5, 1847-1859. Doi: 10.5194/amt-5-1847-2012.

Yom Tov, Y., Ashkenazi, S., Viner, O., 1995. Cattle predation by the golden jackal Canis areus in the Golan Heights, Israel. Biol. Conserv. 73, 19-22.

Zinevich, A., Alpert, P., Messer, H., 2008. Estimation of rainfall fields using commercial microwave communication networks of variable density. Adv. Water Resour. 31, 1470-1480.

Zinevich, A., Messer, H., Alpert, P., 2009. Frontal rainfall observation by a commercial microwave communication network. J. Appl. Meteorol. Climatol. 48, 1317-1334.

Zinevich, A., Messer, H., Alpert, P., 2010. Prediction of rainfall intensity measurement errors using commercial microwave communication links. Atmos. Meas. Tech. 3, 1385-1402.

Ziv, B., 2001. A subtropical rainstorm associated with a tropical plume over Africa and the Middle East. Theor. Apply. Climatol. 69, 91-102.

Figures
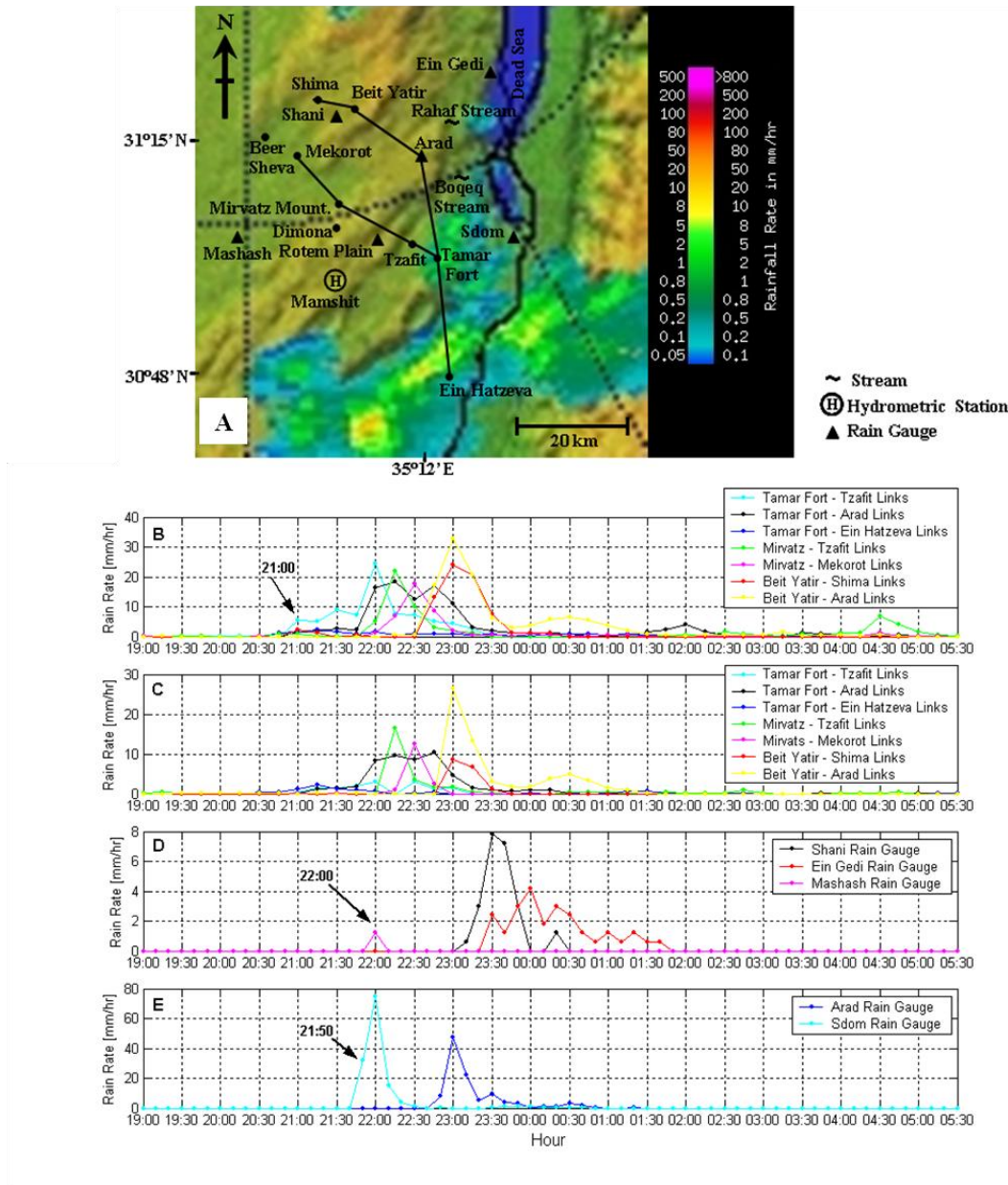
Fig. 1. The microwave links and rain gauges located in the arid region are superimposed over a magnified radar image (A) which was acquired at 21:00 LT.(B)-(E): Maximal (B) and minimal (C) intensities of precipitation as measured by the microwave links, compared to that measured by the IMS' rain gauges (Fig. (D) and (E)) located in the area. The Rotem plain rain gauge, not depicted here, did not measure precipitation at all. The indicated time represents the first detection of precipitation. The color of each convective cell indicates the rainfall intensity according to the scale found to the right of each image.
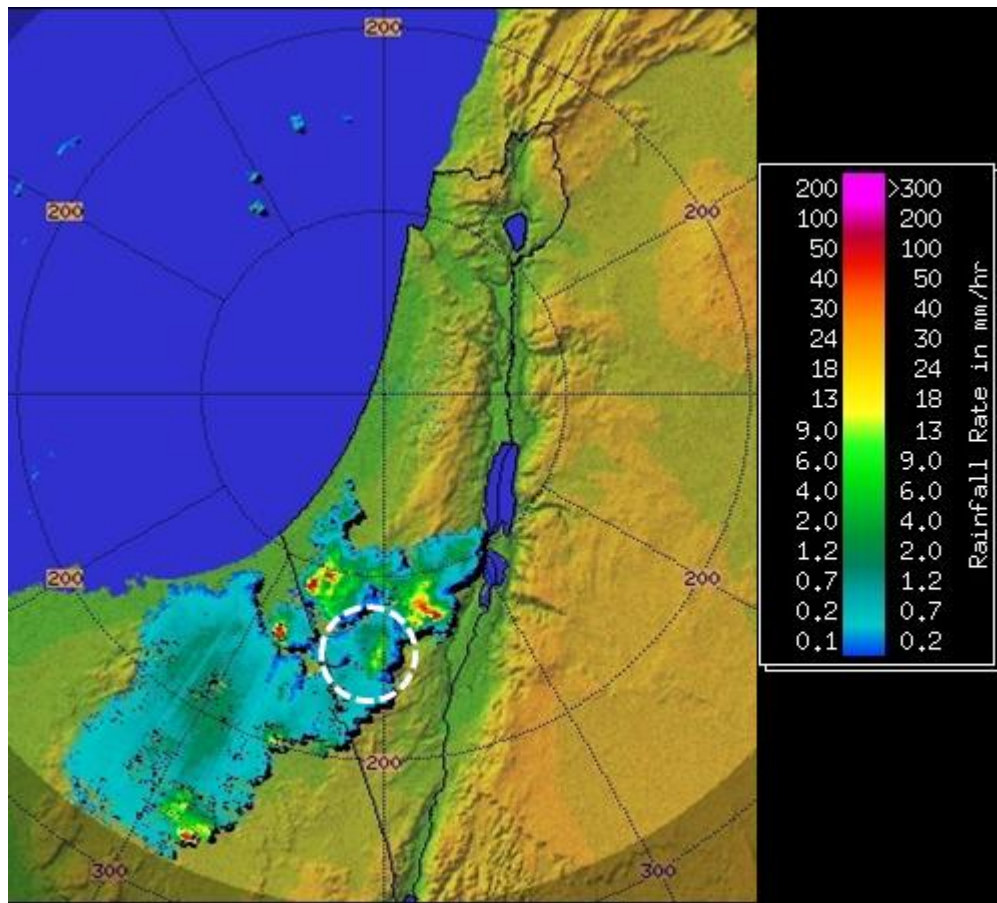
Fig. 2. The IMS radar image which was taken at 19:00 LT during January 17. The study area is marked by a circle. The radar measurements from this region are taken at an altitude of about 2 km above the ground.
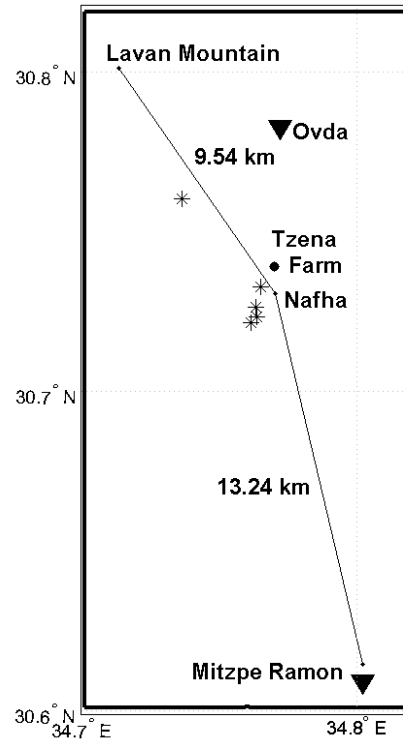
Fig. 3. **The microwave links in the site at the northern Negev. The physical paths of the 4 links are marked as lines while the two Meteorological Service rain gauges, are denoted by triangles. As a result of the strong rainfall, most of a farm located in the area, was severely damaged. Of some 80,000 m^2 of vineyards, only 9,000 m^2 remained- the damaged centers are indicated by asterisks.**
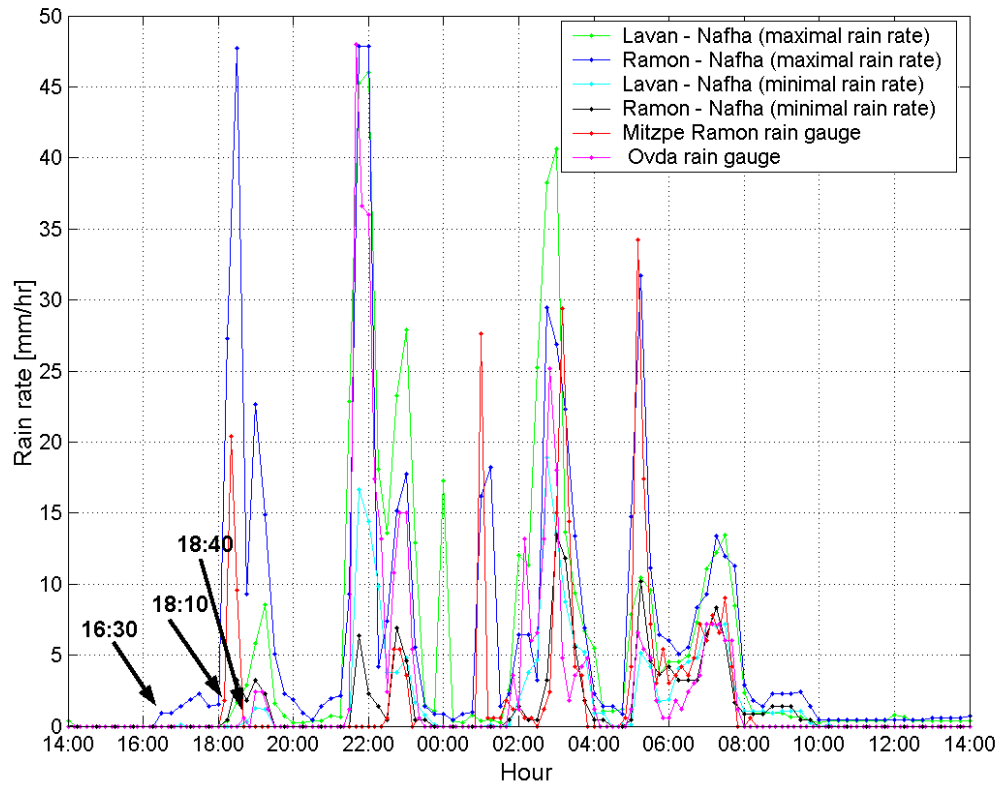
Fig. 4. The maximal and minimal rainfall intensities measured using the microwave links compared to the Mitzpe Ramon and Ovda rain gauges readings. The indicated times (in LT) over the plot denote the first detection of precipitation by the microwave links (16:30) and rain gauges (18:10, 18:40, respectively).
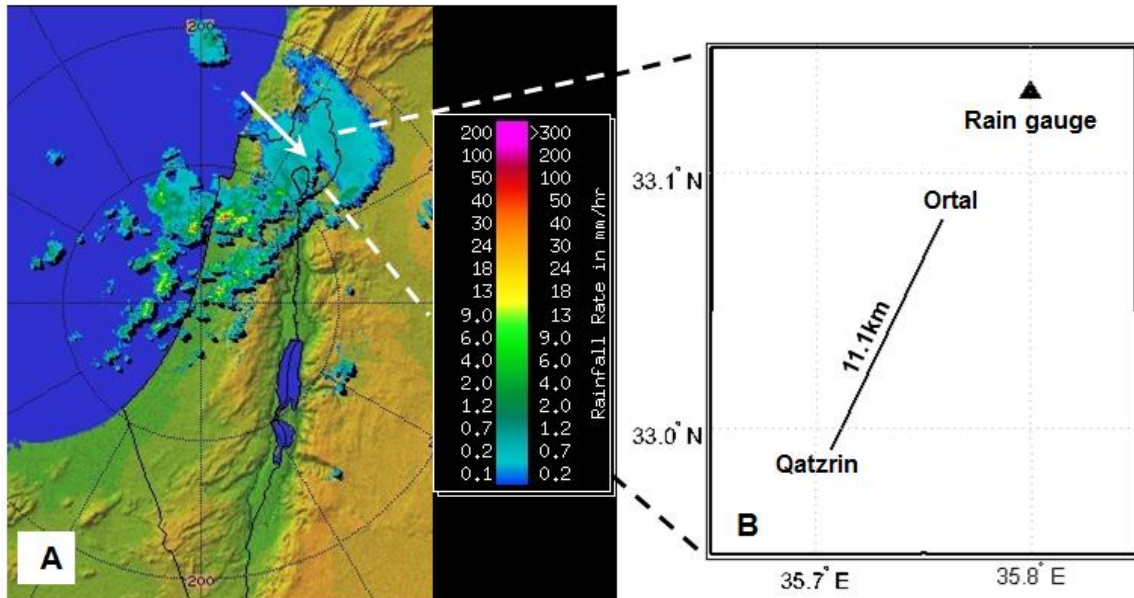
Fig. 5. The IMS radar image (A) was acquired at 13:00 LT. The radar measurements underestimate the precipitation intensity at the Golan Heights region (the area is marked with an arrow). Rain rates of the order of only ~1 mm/hr were measured by this system over the whole area. The IMS rain gauge and microwave links locations at the Golan Heights region (B). Measurements were taken by 2 different microwave links, located across a single physical path (11.1 km long) found at northeastern Israel. Links are installed, along the topographic slope of the area, between 405 m and 923 m above sea level. The IMS rain gauge is located 6.5 km from the northern end of the links at an elevation of 950 m above sea level.

26
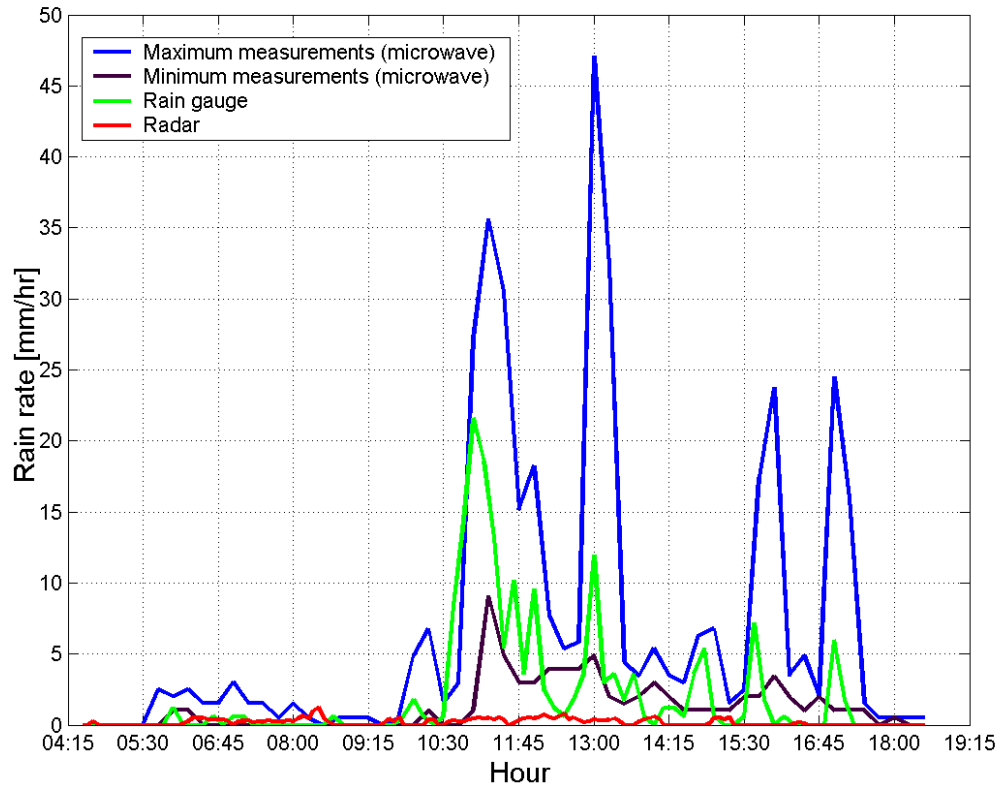
Fig. 6. The minimal and maximal microwave links measurements (in black and blue, respectively) taken on 11 December 2010 between 04:30 to 18:30 LT. The system provides measurements every 15 minutes with a quantization error of 1 dB. System frequency range: 18-19 GHz. Also presented are rain gauge measurements (green) and radar observations (red). Rain gauge measurements can be seen to fall between the minimum and maximum QPE of the links while radar observations are of up to ~1 mm/hr during the entire event.